ポプレックスの表面状態は表面電位で評価されてきたが、ここではPEG修飾によるリポソームとリポプレックスの表面水和状態を測定し、その細胞内取り込み及び遺伝子発現への影響を調べた。

まず、カチオン性脂質としてコレステロール誘導体（OH-Chol）からなるリポソームやそのリポプレックスの水和状態は、PEG脂質の添加によってGP値は変化しなかったが、誘電緩和時間は高くなり、水和する傾向を示した。OH-Cholの二級アミノ基の解離状態がPEGによって遮蔽されるためGP値に変動がなかったと推察された。リポプレックスの水の誘電緩和時間と細胞内取り込み量は負の相関性が見られた（R=0.946）。

DOTAPからなるリポソームやそのリポプレックスの水和状態は、GP値と誘電緩和時間からも、PEG修飾が増加すると水和する傾向がみられた。しかし、このリポプレックスでは、水和しても細胞内取り込みは高くなった。この場合はGPでも水和状態が測定できたことより、PEGのリポソーム表面での運動性が低いと考えられ、リポソームの表面にある正電荷によって細胞内に取り込まれたと推察した。

リポソームとリポプレックスのGP値と誘電緩和時間を比較すると、どちらの測定値からもリポプレックスになると、脱水和することがわかった。

GP値は蛍光物質の分布するカチオン性脂質の極性基近傍の水和状態を反映している。誘電緩和時間は溶液中の水分子の平均の動きを反映していており、カチオン性脂質の極性基に水和した水分子とPEG鎖に水和した水分子も緩和時間の増加に寄与していると推察される。したがって、リポソーム全体の水和状態を反映すると考えられる。

E．結論

水の誘電緩和測定によって蛍光プローブを用いた方法(GP測定)と同様にPEG修飾リポソームの水和状態が測定できること、PEGの表面状態がリポプレックスの細胞内取り込みに影響することが明らかとなった。リポソーム表面でのPEGのマッシュルーム・ブラシ分布状態もGP測定と水の誘電緩和測定によって、推定できることが示唆された

F．健康危険情報

なし

G．研究発表

1．論文発表

1) Y. Iwase, Y. Maitani, Dual functional octreotide-modified liposomal irinotecan leads to high therapeutic efficacy for medullary thyroid carcinoma xenografts. Cancer Sci.103(2):310-6 (2012).

2) Shiraishi K, Harada Y, Kawano K, Maitani Y, Hori K, Yanagihara K, Takigahira M, Yokoyama M. Tumor Environment Changed by Combretastatin Derivative (Cderiv) Pretreatment That Leads to Effective Tumor Targeting, MRI Studies, and Antitumor Activity of Polymeric Micelle Carrier Systems. Pharm. Res. Pharm Res. 29(1):178-86 (2012).

3) FT Fatema, Y. MAITANI, T. AKAIKE, mRNA delivery through fibronectin associated liposome-apatite particles: a new approach for enhanced mRNA transfection to mammalian cell, Biol. Pharm. Bull,35(1):111-5 (2012).

4) Y. Hattori, Y. Nagaoka, M. Kubo, H. Yamasaku , Y. Ishii, H. Okita , H. Nakano, S. Uesato, Y. Maitani, Antitumor effect of liposomal histone deacetylase inhibitor-lipid conjugates in vitro, Chem. Pharm. Bull. 59(11) 1386-1392 (2011).

5) A. Wakasugi , M. Asakawa, M. Kogiso, T. Shimizu, M. Sato, Y. Maitani, Organic nanotubes for drug loading and cellular delivery. Int J Pharm. 413(1-2):271-278 (2011)..

6) Y. Iwase, Y. Maitani, Octreotide-targeted liposomes loaded with CPT-11 enhanced cytotoxicity for the treatment of medullary thyroid carcinoma in vitro, Molecular Pharmaceutics, 8(2):330-337 (2011).

7) Y. Maitani, PEGylated lipidic systems with prolonged circulation longevity for drug

delivery in cancer therapeutics, Journal of Drug Delivery Science and Technology, 21, 27-34 (2011)

8) K. Kawano, Y. Maitani, Effects of polyethylene glycol spacer length and ligand density on folate receptor targeting of liposomal doxorubicin in vitro, J Drug Delivery, 160967 (2011)

9) Y. Harada, T. Yamamoto, M. Sakai, T. Saiki, K. Kawano, Y. Maitani and M. Yokoyama, Effects of organic solvents on drug incorporation into polymeric carriers and morphological analyses of drug-incorporated polymeric micelles. Int J Pharm. 404(1-2):271-280 (2011)..

10) T. Izumisawa, Y. Hattori, M. Date, K. Toma, Y. Maitani, Cell line-dependent internalization pathways determine DNA transfection efficiency of decaarginine-PEG-lipid, Int J Pharm. 404: 264–270 (2011).

2. 学会発表

1) 田中拓海，服部喜之，米谷芳枝 アンギオテンシン II 昇圧下におけるリポプレックスの腫瘍内分布 日本薬学会　第 131 年会(2011.3)

2) 加藤真子，服部喜之，米谷芳枝 コラゲナーゼ処理による静脈内投与したリポプレックスの腫瘍集積性及び遺伝子発現への影響 日本薬学会　第 131 年会(2011.3)

3) 玉井理大，川野久美，米谷芳枝 Sunitinib 封入正電荷リポソームの調整と抗腫瘍効果の評価 日本薬学会　第 131 年会(2011.3)

4) 山作晴香，服部喜之，米谷芳枝　がん遺伝子導入用負電荷ポリマー被覆リポプレックス製剤の開発 日本薬剤学会　第 26 年会(2011.5)

5) 岩瀬由布子，米谷芳枝 イリノテカン封入オクトレオチド修飾ナノ粒子製剤による甲状腺髄様がん治療効果 日本薬剤学会　第 26 年会(2011.5)

6) 山口美智子，内藤陽子，青枝大貴，石井健，白石貢一，横山昌幸，米谷芳枝 Rhodamine 標識PEG 修飾リポソームによるABC 現象誘導の解明第27回日本DDS学会学術集会(2011.6)

7) 中村由梨，昆真生，眞田絵実，浅川真澄，小木曽真樹，清水敏美，米谷芳枝 イリノテカン封入オーガニックナノチューブを用いた非球形キャリアーの体内分布の評価 27 回日本 DDS 学会学術集会(2011.6)

8) Haruka Yamasaku, Yoshiyuki Hattori, Yoshie Maitani Enhanced tumor transfection after systemic injection of lipoplex coated with anionic polymers 38th Annual Meeting & Exposition of the Controlled Release Society(2011.7)

9) 服部喜之，加藤真子，久保愛美，米谷芳枝 コラゲナーゼ処理した担がんマウスにおけるリポプレックスの腫瘍集積性及び遺伝子発現 アンチセンス・遺伝子・デリバリー シンポジウム　2011(2011.9)

10) 中村司，服部喜之，大野浩章，藤井信孝，米谷芳枝 新規正電荷コレステロール誘導体を用いたナノ粒子製剤の前立腺がんに対する遺伝子導入効率の評価 アンチセンス・遺伝子・デリバリー シンポジウム　2011(2011.9)

11) Y. Maitani Functional nanoparticles for cancer therapy 18th International Symposium on Microcapsulation(2011.9)

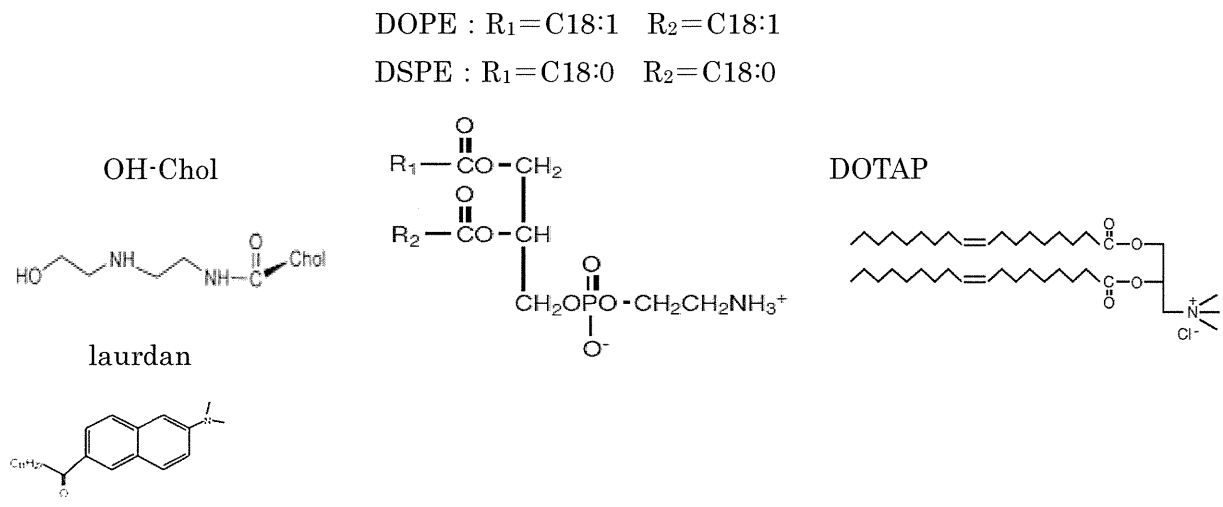

Fig. 1 Chemical structures of lipids and laurdan

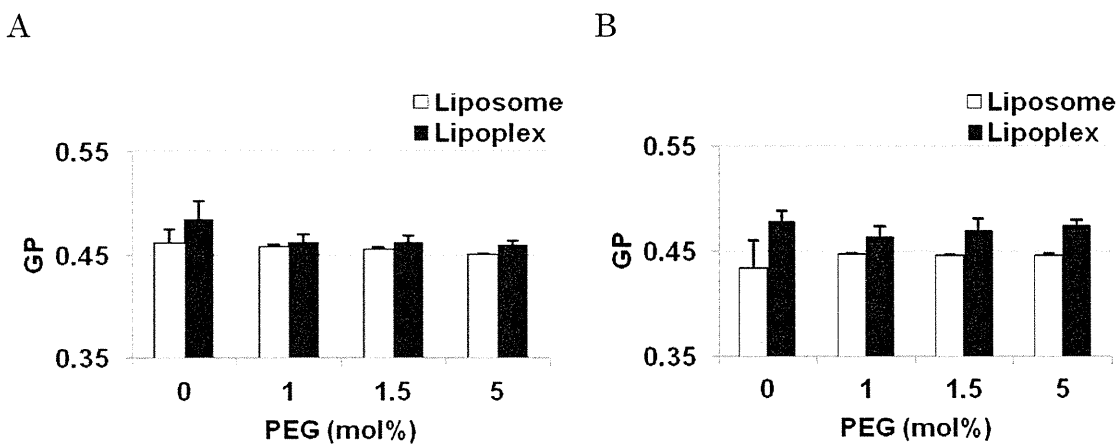

Fig. 2 The change of surface hydration of PEGylated OH-Chol/DOPE-liposome and lipoplex by PEGylation amount as monitored by laurdan generalized polarization (GP) in PBS (A) and water (B) at a charge ratio of (+/-) 3.

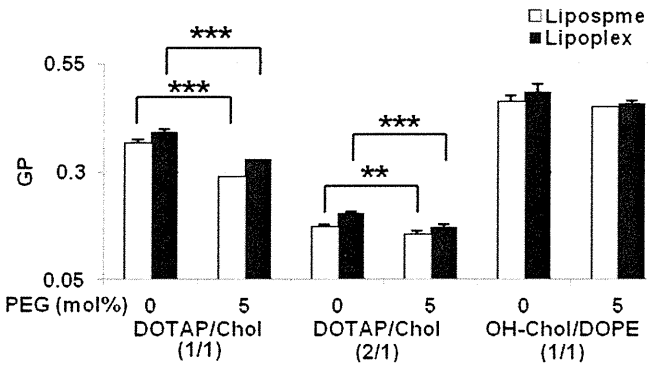

Fig. 3 The change of surface hydration of PEGylated liposome and lipoplex by PEGylation amount as monitored by laurdan generalized polarization (GP) in PBS at a charge ratio of (+/-) 3

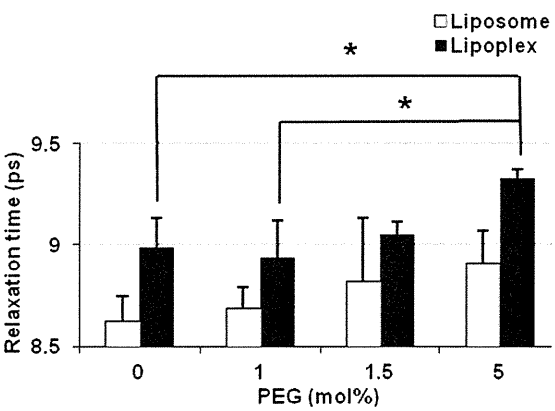

Fig. 4 Dielectric relaxation of OH-Chol/DOPE (1/1) liposomes and their lipoplexes in Milli-Q water

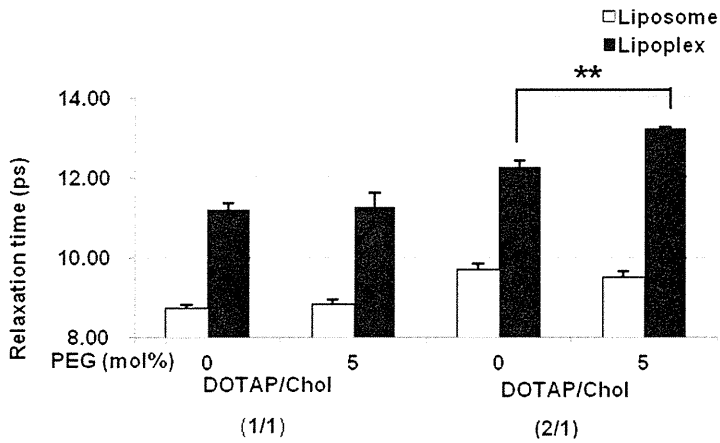

Fig. 5 Dielectric relaxation of DOTAP/Chol (1/1),(2/1) liposomes and their lipoplexes in Milli-Q water

A

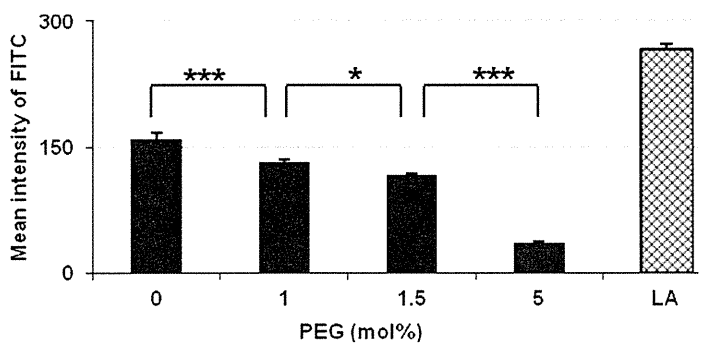

B

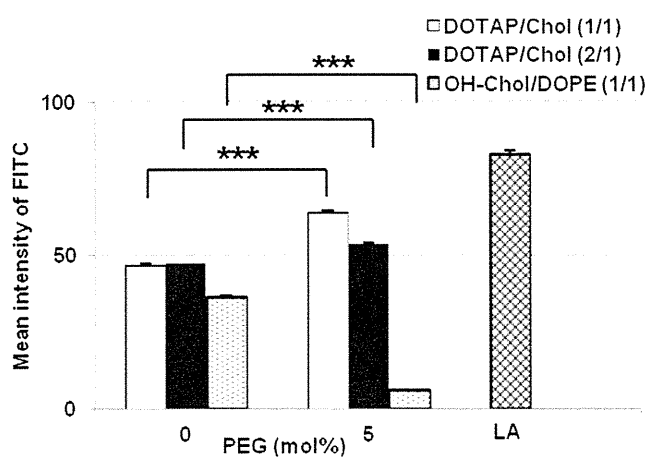

Fig. 6 Cellular association of FITC-DNA of PEGylated OH-Chol-liposomes (A) and DOTAP/Chol (1/1),(2/1) liposomes (B) at a charge ratio of (+/-) 3. Each result represents the mean±S.D. (n=3). *** $P<0.001$ and * $P<0.05$.

別添５

研究成果の刊行に関する一覧表

書籍							
著者氏名	論文タイトル	書籍全体の編集者名	書籍名	出版社名	出版地	出版年	ページ
該当なし							

雑誌					
発表者氏名	論文タイトル	発表誌名	巻号	ページ	出版年
Yoshie Maitania, Ayako Nakamuraa, Takumi Tanaka, Yukio Aso	Hydration of surfactant-modified and PEGylated cationic cholesterol-based liposomes and corresponding lipoplexes by monitoring a fluorescent probe and the dielectric relaxation time.	Int. J. Pharm.	427	372-378	2012
S. Yoshioka, K.M. Forney, Y. Aso, M.J. Pikal	Effect of sugars on the molecular motion of freeze-dried protein formulations reflected by NMR relaxation times.	*Pharm. Res.*	28	3237-3247	2011
宮崎玉樹、阿曽幸男	熱分析による非晶質医薬品の結晶化の評価	*熱測定*	38	125-131	2011
Tamaki Miyazaki, Yukio Aso, Toru Kawanishi	Feasibility of atomic force microscopy for determining crystal growth rates of nifedipine at the surface of amorphous solids with and without polymers.	*J. Pharm. Sci*	100	4413-4420	2011
阿曽幸男，太田鋼，宮崎玉樹，川西　徹	医薬品添加剤の結晶化度測定法に関する研究	*医薬品医療機器レギュラトリーサイエンス*	42	540-545	2011
Y. Iwase, Y. Maitani	Dual functional octreotide-modified liposomal irinotecan leads to high therapeutic efficacy for medullary thyroid carcinoma xenografts.	*Cancer Sci.*	103 (2)	310-6	2012
Shiraishi K, Harada Y, Kawano K, Maitani Y, Hori K, Yanagihara K, Takigahira M, Yokoyama M.	Tumor Environment Changed by Combretastatin Derivative (Cderiv) Pretreatment That Leads to Effective Tumor Targeting, MRI Studies,	*Pharm. Res.* Pharm Res.	29(1)	178-86	2012

	and Antitumor Activity of Polymeric Micelle Carrier Systems.				
FT Fatema, Y. MAITANI, T. AKAIKE	mRNA delivery through fibronectin associated liposome-apatite particles: a new approach for enhanced mRNA transfection to mammalian cell,	*Biol. Pharm. Bull.*	35(1)	111-5	2012
Y. Hattori, Y. Nagaoka, M. Kubo, H. Yamasaku , Y. Ishii, H. Okita , H. Nakano, S. Uesato, Y. Maitani	Antitumor effect of liposomal histone deacetylase inhibitor-lipid conjugates in vitro,	*Chem. Pharm. Bull.*	59(11)	1386-1392	2011
A. Wakasugi , M. Asakawa, M. Kogiso, T. Shimizu, M. Sato, Y. Maitani	Organic nanotubes for drug loading and cellular delivery.	*Int J Pharm.*	413(1-2)	271-278	2011
Y. Iwase, Y. Maitani	Octreotide-targeted liposomes loaded with CPT-11 enhanced cytotoxicity for the treatment of medullary thyroid carcinoma in vitro.	*Molecular Pharmaceutics*	8(2)	330-337	2011
Y. Maitani	PEGylated lipidic systems with prolonged circulation longevity for drug delivery in cancer therapeutics,	*Journal of Drug Delivery Science and Technology*	21	27-34	2011
K. Kawano, Y. Maitani	Effects of polyethylene glycol spacer length and ligand density on folate receptor targeting of liposomal doxorubicin in vitro,	*J Drug Delivery*	160	967	2011
Y. Harada, T. Yamamoto, M. Sakai, T. Saiki, K. Kawano, Y. Maitani and M. Yokoyama	Effects of organic solvents on drug incorporation into polymeric carriers and morphological analyses of drug-incorporated polymeric micelles.	*Int J Pharm.*	404(1-2)	271-280	2011
T. Izumisawa, Y. Hattori, M. Date, K. Toma, Y. Maitani	Cell line-dependent internalization pathways determine DNA transfection efficiency of decaarginine-PEG-lipid.	*Int J Pharm*	404	264–270	2011

研究成果の刊行物・別刷

International Journal of Pharmaceutics 427 (2012) 372–378

Contents lists available at SciVerse ScienceDirect

International Journal of Pharmaceutics

journal homepage: www.elsevier.com/locate/ijpharm

Hydration of surfactant-modified and PEGylated cationic cholesterol-based liposomes and corresponding lipoplexes by monitoring a fluorescent probe and the dielectric relaxation time

Yoshie Maitani [a,*], Ayako Nakamura [a], Takumi Tanaka [a], Yukio Aso [b]

[a] Institute of Medicinal Chemistry, Hoshi University, Ebara 2-4-41, Shinagawa-ku, Tokyo 142-8501, Japan
[b] National Institute of Health Science, 1-8-1 Kamiyoga, Tokyo 158-8501, Japan

ARTICLE INFO

Article history:
Received 30 September 2011
Received in revised form 30 January 2012
Accepted 9 February 2012
Available online 18 February 2012

Keywords:
Cationic liposome
Cellular association
Dielectric relaxation time
Hydration
Laurdan
Lipoplex
PEGylation

ABSTRACT

For the optimization of plasmid DNA (pDNA)-cationic lipid complexes and lipoplex delivery, proper indexes of the physicochemical properties of lipoplexes are required. In general, the characteristics of lipoplexes are defined by particle size and zeta-potential at various mixing ratios of cationic liposomes and pDNA. In this study, we characterized the hydration level of surfactant-modified and PEGylated cationic cholesterol-based (OH-Chol) liposomes and their lipoplexes by monitoring both the fluorescent probe laurdan and the dielectric relaxation time. Fluorescence measurement using laurdan detected hydration of the headgroup of lipids in surfactant-modified liposomes and PEGylated DOTAP-liposomes, but hardly any fluorescence was detected in PEGylated OH-Chol-liposomes because the PEG layers may extend and cover the fluorescent maker. On the other hand, the measurement of dielectric relaxation time of water molecules revealed total hydration, including hydration of the PEG layer and the headgroup of cationic lipids. Furthermore, we found an inverse correlation between hydration level and cellular uptake of PEGylated lipoplexes ($R = 0.946$). This finding indicated that the dielectric relaxation time of water molecules provides an important indicator of hydration of liposome and lipoplexes along with the fluorescence intensity of laurdan.

1. Introduction

Plasmid DNA (pDNA) is now widely employed in gene therapeutic applications. However, a major obstacle to the clinical application of pDNA is its inefficient cellular uptake. One promising clinical delivery strategy involves the use of pDNA-cationic liposome complexes, known as lipoplexes, in which negatively charged pDNA binds electrostatically to cationic lipids, such as OH-Chol and DOTAP, in liposomes. Such lipoplexes form when cationic liposomes, frequently containing a neutral co-lipid as a helper lipid, such as DOPE, at a 1:1 molar ratio, are mixed with pDNA (Yang and Huang, 1997). Furthermore, to enhance gene delivery, surface modification of the liposomes with surfactants and polymers has been reported. We and Inoh et al. (Inoh et al., 2001; Igarashi et al., 2006) have reported previously that biosurfactant mannosylerythritol lipid-A (MEL-A)-modified liposomes increased gene transfection efficiency in vitro. In in vivo gene delivery, poly(ethylene glycol) (PEG) polymer coating, PEGylation, has been reported frequently because colloidal particles, such as liposomes may be completely lost because of the capture of liposomes by macrophages in the liver and spleen (Blume and Cevc, 1990; Klibanov et al., 1990). PEGylation reduces the extent of uptake by macrophages and enhances the circulation time of liposomes in blood (Woodle et al., 1992; Allen et al., 1995). The underlying mechanism of the stabilization has been explained mainly through hydrated PEG chains on the surface.

In the optimization of lipoplex delivery, indexes of the physicochemical properties of lipoplexes are required. In general, the characteristics of lipoplexes are defined by particle size and zeta-potential at various mixing ratios of cationic liposome and pDNA. The hydration level of surface-modified and PEGylated liposomes has rarely been reported. A semi-quantitative approach for determining changes in the generalized polarization (GP) of laurdan was recently used successfully to characterize changes in hydration at lipid–water interfaces (Meidan et al., 2000). Measurement of dielectric relaxation time provides information on the structure of the hydration layer of colloids that interact with water

Abbreviations: OH-Chol, cholesteryl-3β-carboxyamindoethylene-*N*-hydroxyethylamine; DOPE, dioleoylphosphatidylethanolamine; DOTAP, dioleoyl-3-trimethylammonium propane; DSPE, distearoylphosphatidylethanolamine; DSPE-PEG2000, DSPE-polyethyleneglycol molecular weight 2000; MEL-A, mannosylerythritol lipid-A.

* Corresponding author. Tel.: +81 3 5498 5048; fax: +81 3 5498 5048.
E-mail address: yoshie@hoshi.ac.jp (Y. Maitani).

0378-5173/$ – see front matter © 2012 Elsevier B.V. All rights reserved.
doi:10.1016/j.ijpharm.2012.02.018

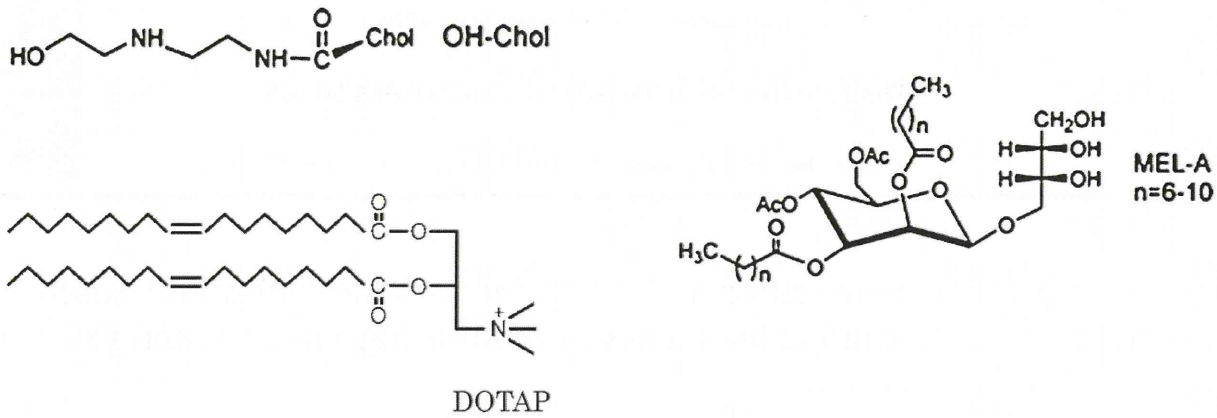

Fig. 1. Chemical structures of cholesteryl-3β-carboxyamindoethylene-*N*-hydroxyethylamine (OH-Chol), dioleoyl-3-tri-methylammonium propane (DOTAP) and mannosylerythritol lipid-A (MEL-A).

(Sato et al., 2007). In addition, the interactions of polar probe molecules with different environments present in such systems can be investigated. The process of dipolar relaxation may be related to the number of water molecules around the fluorescent moiety of laurdan. To the best of our knowledge, this is the first study to characterize the hydration of surfactant-modified and PEGylated cationic cholesterol-based liposomes and lipoplexes by measurement of dielectric relaxation time and to make a comparison with the GP value.

In this study, liposomes (~130 nm diameter) composed of either OH-Chol/DOPE/MEL-A (molar ratio 1:1:1) or OH-Chol/DOPE/Tween 80 (molar ratio 1:1:0.5) were employed as a model of surfactant-modified cationic cholesterol-based liposomes. PEGylated liposomes (~140 nm diameter) composed of OH-Chol/DOPE/DSPE/DSPE-PEG2000 (molar ratio 1:1:x:0.1−x) or DOTAP/Chol/DSPE/DSPE-PEG2000 (molar ratio 1:1:x:0.4−x) were employed as a model of PEGylated cationic cholesterol-based liposomes.

The present study aimed to examine the impact of surfactant-modification and PEGylation on the hydration of liposome and their lipoplexes by both monitoring lipid hydration level by the emission characteristics of the fluorescent probe laurdan included in the lipid bilayer and measurement of the dielectric relaxation time. Furthermore, the relationship between hydration of PEGylated lipoplexes, cellular association and transfection efficiency was investigated.

2. Materials and methods

2.1. Materials

OH-Chol was synthesized as reported previously (Fig. 1) (Takeuchi et al., 1996; Hattori et al., 2005). DOPE, Tween 80, DSPE and DSPE-PEG2000 (DSPE-PEG) were obtained from NOF Co., Ltd. (Tokyo, Japan), and MEL-A was purified as reported previously (Kitamoto et al., 1998) (Fig. 1). 6-Dodecanoyl-2-demethylaminonaphthalene (laurdan) was purchased from Lambda (Graz, Austria). DOTAP was purchased from Avanti Polar Lipids, Inc. (Alabaster, AL, USA) (Fig. 1). Plasmid DNA (pDNA), encoding the luciferase gene was constructed as described previously (Igarashi et al., 2006). A protein-free preparation of pDNA was purified following alkaline lysis using Maxiprep columns (Qiagen, Hilden, Germany). Fluorescein-labeled pDNA (FITC-DNA) was synthesized using pDNA and a fluorescein labeling kit (Mirus, Madison, WI, USA). Lipofectamine 2000 (Lipofectamine) was purchased from Invitrogen Corp. (Carlsbad, CA, USA).

2.2. Preparation of liposomes and lipoplexes

OH-Chol was formulated into liposomes with DOPE at a molar ratio of 1/1, and MEL-A or Tween 80 as a surfactant (OH-Chol/DOPE/surfactant = 1:1:1 or 1:1:0.5, respectively), which were prepared by a modified ethanol injection method (Hattori et al., 2005) with a cationic lipid concentration of 4.5 mM. The formulations were as reported previously (Ding et al., 2009a). Two kinds of PEGylated liposomes were formulated with OH-Chol or DOTAP as cationic lipids and designated OH-Chol-liposomes (OH-Chol/DOPE/DSPE/DSPE-PEG = 1:1:x:0.1−x) and DOTAP-liposomes (DOTAP/Chol/DSPE/DSPE-PEG = 1:1:x:0.4−x, molar ratio), respectively, prepared by a dry film method with a cationic lipid concentration of 4.5 mM. DSPE was used to compensate for changes in lipid membrane fluidity and electric charge by the addition of PEG-DSPE. The size of liposomes was adjusted by sonication with bath-typed sonicator. Here, unspecialized cationic liposomes indicate OH-Chol-liposomes.

To measure the hydration level of the liposomal surface, 0.2% (molar % to total lipids) laurdan was incorporated into the lipids. Lipoplexes at a charge ratio (+/−, amine in cationic lipids/pDNA phosphate ratio) of 3 or 5 were prepared by adding an aliquot of pDNA to each liposome mix and standing at room temperature for 5 min.

The size and zeta-potential of liposomes and lipoplexes were measured using an ELS-Z2 (Otsuka Electronics Co., Ltd., Osaka, Japan) in Milli Q water (water) (Elix® equipment, Millipore, MA, USA) or 1/10 phosphate-buffered saline (pH 7.4, 1/10 PBS).

2.3. Generalized polarization (GP) measurement

Twenty microliters of 0.2 mol% laurdan-labeled liposomes were diluted to 2 mL with PBS to a cationic lipid concentration of 0.045 mM. Lipoplexes were prepared by adding 40.8 μL liposomes to 59.2 μL pDNA (20 μg/mL of pDNA) and incubating for 5 min. After 20 μL of lipoplexes were diluted to 2 mL with PBS or water to a cationic lipid concentration of 0.0186 mM with 0.2 μg/mL of pDNA, laurdan fluorescence was measured by scanning emission wavelengths between 440 and 490 nm with an excitation wavelength of 340 nm (bandwidth 5 nm) at 25 °C in a Shimadzu RF-5300PC, as reported previously (Ding et al., 2009a). Cationic lipid concentrations of liposome (0.019–0.045 mM) increased GP values slightly with the increase in lipid concentration. Spectra were obtained at 0 min (not specially described) and at 30 min after dilution of the lipoplex mix with water or PBS. Laurdan is a membrane probe highly sensitive to environmental polarity, and it displays a large

red shift in emission in polar solvents with respect to nonpolar solvents (Parasassi et al., 1991). It is possible to follow the interfacial water changes in the cationic liposomes upon their complexation with pDNA by means of the spectral variations of laurdan (Parasassi et al., 1991) and by calculating the GP value as follows:

$$GP = \frac{(I_{440} - I_{490})}{(I_{440} + I_{490})} \quad (1)$$

wherein I_{440} and I_{490} are the emission intensities at wavelengths of 440 nm and 490 nm, respectively, with an excitation wavelength of 340 nm (Parasassi et al., 1991; Hirsch-Lerner and Barenholz, 1999). A higher GP value represents a lower hydration level (dehydration) on the liposomal surface. GP values were calculated from the absolute values of fluorescence intensity from one measurement, which was run in the same day with strictly controlled conditions. The repeated experiments showed different values, but with a similar trend.

The effect of pDNA on the GP value for various cationic liposomes is described as

$$\Delta GP = GP \text{ of lipoplex} - GP \text{ of liposome} \quad (2)$$

2.4. Dielectric relaxation time measurement

Dielectric relaxation time of water molecules was measured using a digitizing oscilloscope (model 54120B, Agilent Technologies) at 25 °C in water as reported previously (Yoshioka et al., 1995). At total lipid concentrations of 10–30 mg/mL, dielectric relaxation time did not change (data not shown); therefore, a total lipid concentration of 11.2 mg/mL, corresponding to 9 mM cationic lipid, was used.

2.5. Transfection protocol and luciferase activity measurement

The human lung adenocarcinoma A549 cell line was kindly provided by OncoTherapy Science. The cells were maintained in RPMI-1640 medium supplemented with 10% FBS and kanamycin (100 mg/mL) at 37 °C in a 5% CO_2 humidified incubator. Cells at a confluence level of 70% in a 22-mm culture dish were transfected with each lipoplex. For transfection, the prepared lipoplexes with 1 μg of pDNA were diluted in 500 μL of culture medium and then incubated with the cells for 24 h. For transfection with Lipofectamine as a control, 2.5 μL of Lipofectamine was used for 1 μg of pDNA to form a complex in Opti-MEM, in accordance with the manufacturer's protocol. Luciferase expression in A549 cells was measured as counts per second (cps)/μg protein using the luciferase assay system (Picagene, Tokyo Ink Mfg. Co., Ltd., Tokyo, Japan) and the cps value was normalized to the protein concentration, as determined using a bicinchoninic acid protein assay (Pierce, Rockford, IL, USA).

2.6. Flow cytometry

A549 cells were prepared by plating in a 35-mm culture dish 24 h prior to each experiment. Each liposome was mixed with 2 μg of FITC-DNA at a charge ratio (+/−) of 3:1, and then diluted in 1 mL of PBS. Cells were incubated with the lipoplexes at 37 °C for 2 h. After incubation, the cells were washed two times with PBS and detached with 0.05% trypsin and centrifuged at 1500 rpm for 3 min. The supernatant was discarded and the cell pellets were resuspended with PBS containing 0.1% BSA and 1 mM EDTA. The suspended cells were introduced directly into a FACSCalibur flow cytometer (Becton Dickinson, CA, USA). Data for 10,000 fluorescent events were obtained by recording forward scatter (FSC), side scatter (SSC), and green fluorescence. Mean intensity values of FITC inside cells were calculated to compare the uptake amount of lipoplexes.

2.7. Statistical analysis

The statistical significance of differences between mean values was determined using Welch's *t*-test. Multiple comparisons were evaluated by analysis of variance (ANOVA) with Tukey's multiple comparison test. *P*-values less than 0.05 were considered significant. All experiments were repeated at least two times.

3. Results and discussion

Previously we reported that lipoplexes of MEL-A-modified liposomes (OH-Chol/DOPE/MEL-A = 1:1:0.5) and Tween 80-modified liposomes showed higher gene transfection efficiency at a charge ratio of (+/−) 3 than at a charge ratio of 5 (Ding et al., 2009b). In addition, the GP value of MEL-A-modified liposomes (OH-Chol/DOPE/MEL-A = 1:1:1) was slightly higher compared with that of liposomes with a lower MEL-A ratio (OH-Chol/DOPE/MEL-A = 1:1:0.5) (Ding et al., 2009a). Therefore, in this study, we used MEL-A-modified liposomes with a 1:1:1 (OH-Chol/DOPE/MEL-A) composition. To examine the hydration levels of MEL-A-modified, Tween 80-modified and PEGylated liposomes, and their lipoplexes, at charge ratios of (+/−) 3 and 5, GP values and dielectric relaxation times were measured and compared.

3.1. Surfactant-modified liposomes and lipoplexes

3.1.1. Size and zeta-potential

The mean particle size of non-modified liposomes and MEL-A- and Tween 80-modified liposomes in water was approximately 130 nm, which was adjusted by sonication. An increase in the charge ratio (+/−) from 3 to 5 increased the zeta-potential of all lipoplexes. In lipoplexes at charge ratios of (+/−) 3 and 5, MEL-A-modified liposomes exhibited a slightly decreased zeta-potential compared with non-modified lipoplexes, but Tween 80 increased it in water (Fig. 2A). These trends were also observed in lipoplexes in 1/10 PBS, although the each zeta-potential was decreased (Fig. 2B). The change in zeta-potential of lipoplexes suggested that the cationic part of OH-Chol was affected by modification of MEL-A and Tween 80.

3.1.2. Hydration monitoring fluorescent probe

The GP value depends mainly on changes in hydration of the bilayer headgroup region either because of changes in the ratio between the less hydrated gel phase and the more hydrated liquid-crystalline phase and gel phase, or because of dependency on the pH in the range 4–10 and the type of polar headgroup (Lerner and Barenholz, 2007).

Fluorescence measurements were undertaken before and after addition of appropriate amounts of pDNA to laurdan-labeled liposomes at charge ratios of (+/−) 3 and 5. The results showed that the mean GP value for liposomes was 0.395 (at a cationic lipid concentration of 0.019 mM) (Fig. 3A). The corresponding values for MEL-A- or Tween 80-modified liposomes were 0.420 and 0.327, respectively (Fig. 3A). MEL-A dehydrated the liposomal surface, while Tween 80 hydrated it, corresponding well with a previous report (Ding et al., 2009a). Because Tween 80 possesses twenty oxyethylene residues in the hydrophilic region, and MEL-A possesses only three hydroxyl groups, the water molecules bound per Tween 80 would be much higher than those per MEL-A (Ding et al., 2009a). Interestingly liposomes and lipoplexes showed the same trend for changes in GP values after surfactant modification.

After pDNA addition, the ΔGP value for the three systems was investigated. Lipoplexes at a charge ratio of (+/−) 3 demonstrated positive ΔGP values, but at a charge ratio of (+/−) 5, lipoplexes showed small negative ΔGP values (Fig. 3B). Positive

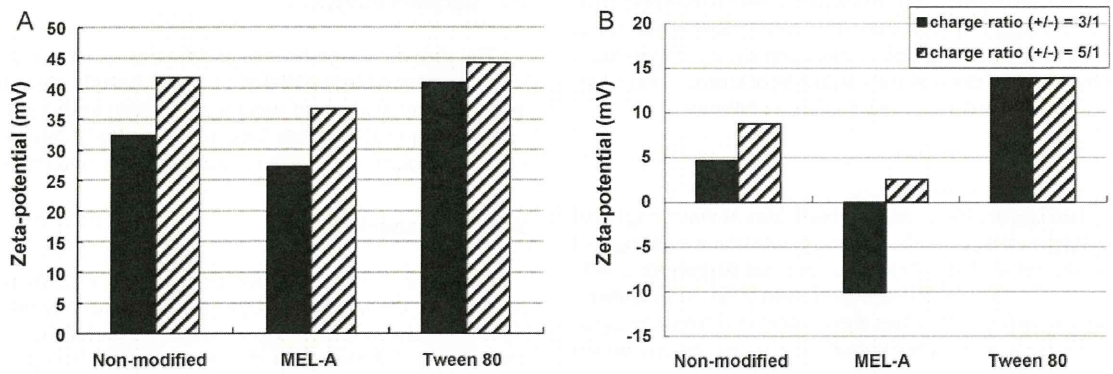

Fig. 2. Zeta-potential of surfactant-modified lipoplexes at charge ratios of (+/−) 3 and 5 in water (A) and 1/10 PBS (B). Each value represents the mean (n = 2).

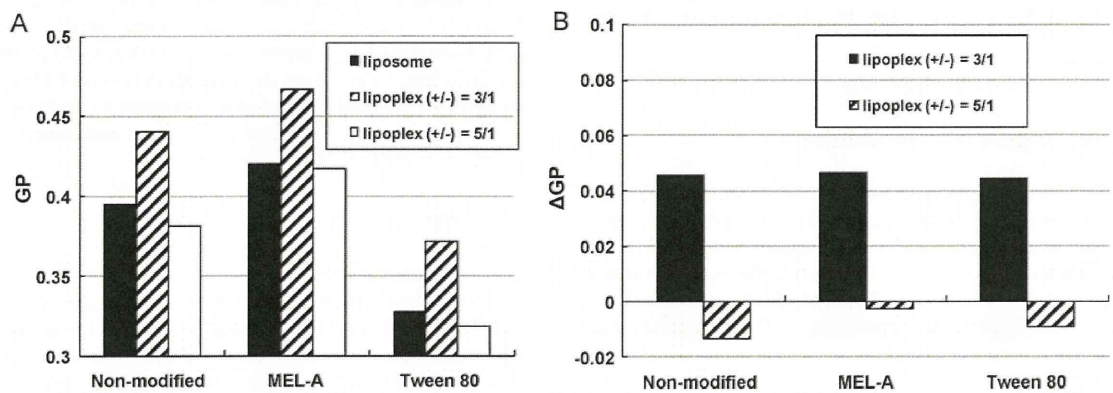

Fig. 3. The change of surface hydration of surfactant-modified liposomes and lipoplexes at charge ratios of (+/−) 3 and 5 as monitored by laurdan generalized polarization (GP) (A) and ΔGP (B) values in PBS. Each value represents the mean (n = 2).

values of ΔGP indicate lower hydration levels than the corresponding liposome formulations (Hirsch-Lerner and Barenholz, 1999; Meidan et al., 2000), i.e. the interaction of cationic lipids with pDNA reduced hydration at the water–lipid interface (Luciani et al., 2007), Negative values of ΔGP indicate that the free headgroups of cationic lipids projected outside of the lipoplex and were hydrated, which indicates excess cationic liposomes. These findings support the increased zeta-potentials of MEL-A- and Tween 80-modified lipoplexes with the increase in charge ratio of (+/−) from 3 to 5. In other words, more positively charged MEL-A- or Tween 80-modified lipoplexes with a charge ratio of (+/−) 5 were more hydrated than those with a charge ratio of (+/−) 3. Hereafter we focus on lipoplexes with a charge ratio of (+/−) 3, where liposomes interact minimally with pDNA.

3.1.3. *Hydration monitoring dielectric relaxation time*

The result of dielectric relaxation time of water molecules in the liposome suspensions revealed that MEL-A-modified liposome exhibited significantly decreased dielectric relaxation times (10.32 ± 0.08 ps) compared with non-modified liposomes (10.87 ± 0.05 ps), and Tween 80-modified liposomes slightly increased it (11.1 ± 0.19 ps) (Fig. 4), indicating dehydration and hydration of liposomes, respectively, compared with non-modified liposomes. Lipoplexes at a charge ratio of (+/−) 3 showed similar trends for dielectric relaxation times compared with liposomes alone. The dielectric relaxation times between liposomes and lipoplexes cannot be compared directly, because hydration of the polar groups of pDNA, such as deoxyribose, is considered to contribute to the dielectric relaxation time of water molecules in lipoplex suspensions.

These findings for GP value and dielectric relaxation time of surfactant-modified liposomes and lipoplexes showed similar trends, indicating that the hydrated outer layer was associated with headgroups of OH-Chol, and pDNA interacts with this part. The change in GP values of liposomes and lipoplexes at a charge ratio of (+/−) 3 indicated that water was excluded from the lipid headgroup region when heterogeneous condensation of cationic lipids by pDNA took place.

As reported previously (Ding et al., 2009a), in terms of the cellular association of surfactant-modified liposomes, the relation of hydration level and zeta-potential to the cellular uptake was not

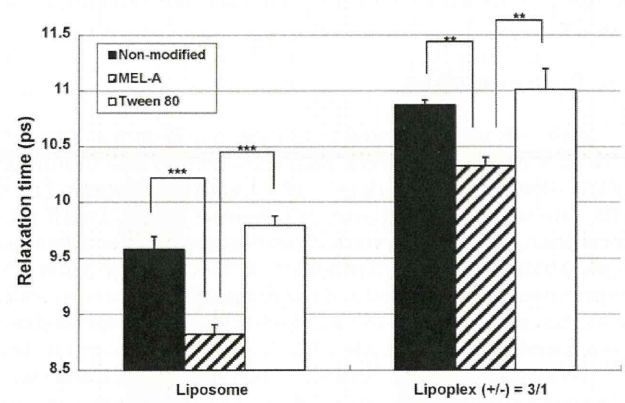

Fig. 4. Dielectric relaxation time of surfactant-modified liposomes and lipoplexes at a charge ratio of (+/−) 3 in water. Data represent mean ± S.D. (n = 3). *P < 0.05, **P < 0.01, ***P < 0.001.

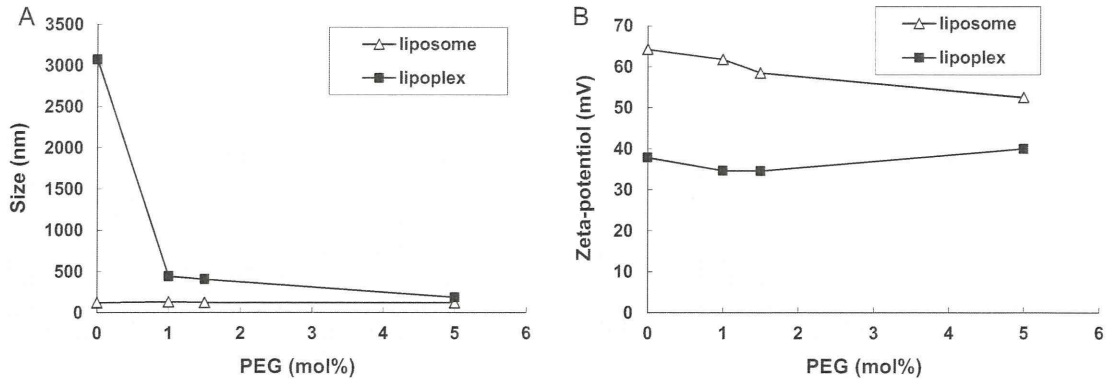

Fig. 5. Size (A) and zeta-potential (B) of PEGylated OH-Chol-liposomes at a charge ratio of (+/−) 3 in water. Each value represents the mean ($n = 2$).

clear for incubation with PBS for 2 h. The ions in PBS might interact with cationic charge on the relatively outer surface of the liposomes even covered with surfactants.

3.2. PEGylated liposomes and lipoplexes

3.2.1. Size and zeta-potential

The particle size and zeta-potentials of OH-Chol-liposomes were 121.9 nm and 64.3 mV, respectively in water (Fig. 5A and B). Without PEGylation, lipoplexes were likely to aggregate. Increasing the amount of PEGylation greatly decreased the lipoplex sizes (Fig. 5A) and did not largely change the zeta-potential of lipoplexes (Fig. 5B). Because the cationic lipid concentration was constant, this change in size is attributed to the packing effects of PEG chains into vesicle structures (Garbuzenko et al., 2005; Sato et al., 2007).

3.2.2. Hydration monitoring fluorescent probe

Next, to examine the effect of PEGylated cationic lipids on GP values, we measured GP values of PEGylated DOTAP-liposome (Fig. 6) and PEGylated OH-Chol-liposome (Fig. 7A). The particle size and zeta-potentials of DOTAP-Chol-liposomes from 0 to 20 mol% were 105.8 ± 1.3–142.7 ± 22.5 nm and 38.3 ± 1.3–45.7 ± 3.0 mV, respectively in water. The fluorescence of liposomes was recorded in PBS. A large decrease in GP values of liposomes at 5 mol% PEG, which are often used for PEGylation of liposomes. From these results, we focused on modification below 5 mol% PEG.

The fluorescence of OH-Chol-liposomes in PBS and lipoplexes was recorded GP and GP (0 min and 30 min) after dilution with PBS, respectively (Fig. 7A). Unlike with PEGylated DOTAP-liposomes, the values of PEGylated OH-Chol-liposome did not decrease largely

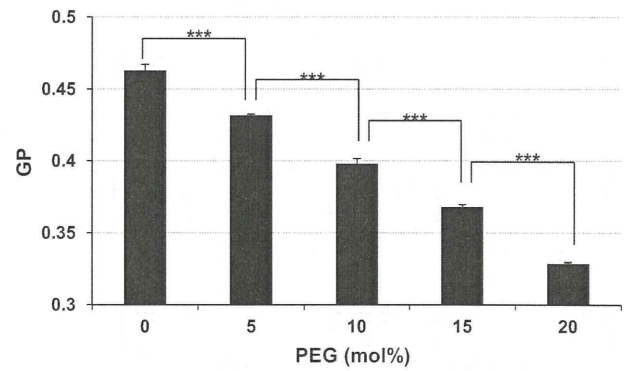

Fig. 6. The change of surface hydration of PEGylated DOTAP-liposome by PEGylation amount as monitored by laurdan generalized polarization (GP) in PBS at a charge ratio of (+/−) 3. Data represent mean ± S.D. ($n = 3$). ***$P < 0.001$.

at 5 mol% PEG. The GP values of OH-Chol-liposomes were higher than those of DOTAP-liposomes for all degrees of PEGylation. That is, PEGylated OH-Chol-liposomes were less hydrated, and PEGylated DOTAP-liposomes were more hydrated, corresponding with a previous report in which cholesterol induced the dehydration of lipid bilayers (Hirsch-Lerner and Barenholz, 1999; Meidan et al., 2000). Stepniewski et al. (2011) reported that PEG penetrates the lipid core of the membrane for the case of a liquid-crystalline membrane but is excluded from the tighter structure of the gel membrane. Because DOTAP-liposomes have more fluid membrane than OH-Chol-liposomes, the difference of changes in GP values by PEGylation may be as a result of the different structures of PEG

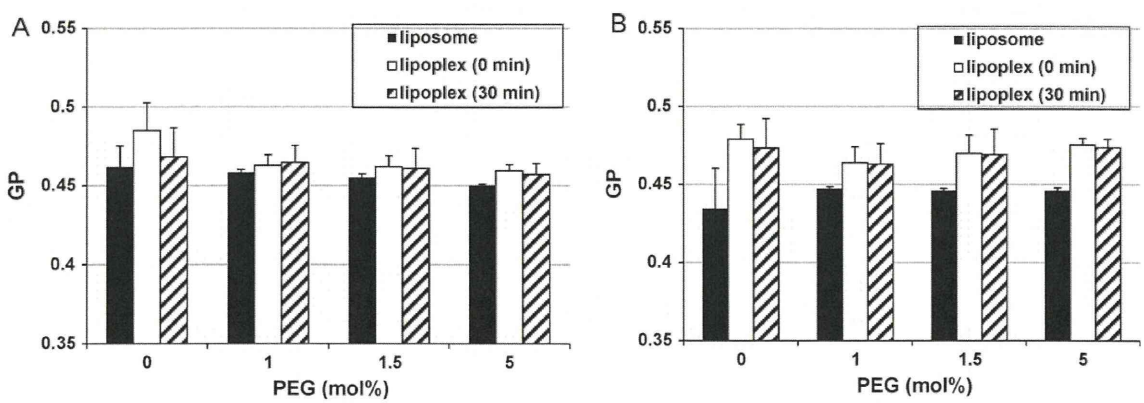

Fig. 7. The change of surface hydration of PEGylated OH-Chol-liposomes and lipoplexes at a charge ratio of (+/−) 3 as monitored by laurdan generalized polarization (GP) 0 min or 30 min after dilution with PBS (A) or water (B). Data represent mean ± S.D. ($n = 3$).

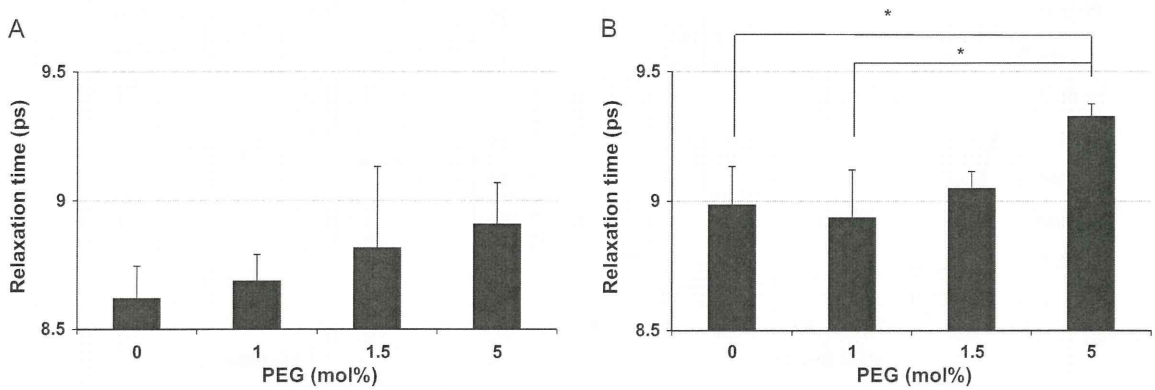

Fig. 8. Dielectric relaxation times of PEGylated OH-Chol-liposomes (A) and lipoplexes (B) at a charge ratio of (+/−) 3 in water. Data represent mean ± S.D. ($n = 3$). *$P < 0.05$.

on the liposomal membrane. PEG layers may cover and extend the fluorescence of laurdan at the headgroups of OH-Chol.

To examine the effect of the solvent on GP values, we also measured GP values of the same liposomes and lipoplexes in water. The GP values of PEGylated OH-Chol-liposomes and lipoplexes in water were similar to those in PBS (Fig. 7B). The GP (0 min and 30 min) values of lipoplexes at a charge ratio of (+/−) 3 hardly changed between PBS and water. The degrees of PEGylation were not reflected change of GP values.

3.2.3. *Hydration monitoring dielectric relaxation time*

Unlike the GP values, the dielectric relaxation times of PEGylated OH-Chol-liposome were longer with increasing amounts of PEG in water, indicating the hydrated PEG layer (Fig. 8A). In addition, the dielectric relaxation times of lipoplexes were significantly longer than those of non-PEGylated and 1 mol% PEGylated lipoplexes (Fig. 8B). These findings indicated that PEGylated liposomes and PEGylated lipoplexes were hydrated with increasing amounts of PEG.

In the present study, we measured dielectric relaxation time in a frequency range between 0.1 GHz and 20 GHz. A dielectric loss peak at approximately 10 GHz was observed for all the suspensions of surface-modified cationic liposomes and lipoplexes studied. The loss peak is considered to be because of the dielectric relaxation of bulk water and the relaxation of water hydrated to PEG and the headgroups of cationic lipid. For PEG and DSPE-PEG solutions, the relaxation time of hydrated water has been reported to be 5–6 times longer than that of bulk water (Sato et al., 2007). In the present study, the dielectric loss peak was not separated into each relaxation process because of the limitations of the measuring frequency of the instrument used (<20 GHz). Therefore, the relaxation time measured in the present study reflected both relaxation processes, and the longer relaxation time indicates a higher contribution of hydrated water of PEG with longer relaxation time than that of bulk water.

The influence of the surface-modification of cationic liposomes by surfactants and PEG-lipid on the hydration level of liposomes and the corresponding lipoplexes were examined by measurement of GP values of a fluorescent marker and of dielectric relaxation. In surfactant-modified liposomes, GP values and dielectric relaxation times demonstrated that liposomes modified with MEL-A and the corresponding lipoplexes were more dehydrated, but liposomes with Tween 80 were more hydrated compared with unmodified liposomes. In PEGylated liposomes, changes in GP values of liposome and lipoplexes were hardly observed at a charge ratio of (+/−) 3. Dielectric relaxation times in water demonstrated that more highly PEGylated liposomes and lipoplexes were more hydrated.

3.2.4. *Cellular association and transfection efficiency of PEGylated lipoplexes*

Finally to clarify the relationship between PEGylation and transfection levels, we examined the cellular association of lipoplexes using FITC-DNA in A549 cells incubated 2 h by flow cytometry. In Fig. 9A, with the presence of PEG-lipid in the lipoplexes, a significant decrease of cellular uptake was in each step from 159.9 ± 7.6 with non-PEGylated lipoplexes to 36.0 ± 0.6 with 5 mol% PEGylated lipoplexes. In accordance with this, the luciferase activity was decreasing roughly 150-fold from 75,444 cps/μg protein with non-PEGylation to 494 cps/μg protein with 5 mol% PEGylated lipoplexes (Fig. 9B).

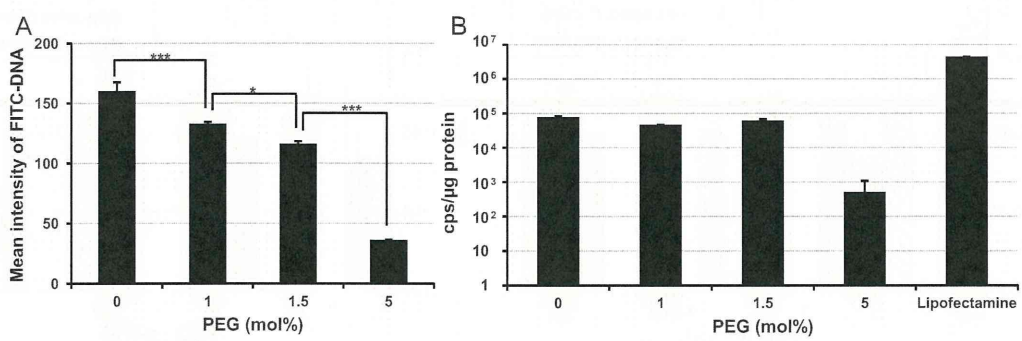

Fig. 9. Cellular association of FITC-DNA (A) and transfection efficiency (B) of PEGylated OH-Chol-liposomes at a charge ratio of (+/−) 3. Lipoplexes were incubated with A549 cells for 2 h in PBS measured by flow cytometry (A) and for 24 h in culture medium for gene transfections (B). Each result represents the mean ± S.D. ($n = 3$). ***$P < 0.001$ and *$P < 0.05$.

We found an inverse correlation between the amount of PEGylation in the lipoplexes and uptake in A549 cells. PEGylation significantly decreased the association of the lipoplexes at 2 h from the FITC intensities, corresponding with the result of DOTAP/cholesterol lipoplexes (Gjetting et al., 2010). The decreased cellular association of lipoplexes by PEGylation was probably caused by the steric barrier of PEG layers where the zeta-potential was not greatly changed by PEGylation between 34.57 and 39.98 mV (Fig. 5B). It was suggested that PEG layers may be projected out of the solid liposomes. In other words, the hydration level of PEG-lipid on liposomes by measurement of dielectric relaxation may reflect the projection level of PEG layers out of liposomes. Transfection efficiencies were not consistent with the result of cellular uptake except for 5 mol% PEGylation. Other factors might affect transfection efficiency more than cellular uptake. Until now, it has been speculated that there is a negative relationship between hydration ratio by PEGylation and cellular uptake of lipoplexes. This is the first study to measure hydration ratio of PEGylated lipoplexes and demonstrate that there is a correlation between hydration level and cellular uptake of PEGylated lipoplexes ($R = 0.946$). This indicates that PEGylation of liposomes may be attributed to hydration more than the cationic headgroups, which were monitored by dielectric relaxation times. Thus, the hydration of lipids is the proper index to evaluate the quality of PEGylated lipoplexes.

4. Conclusions

Fluorescence measurements with laurdan detected the hydration of headgroups of lipids in surfactant-modified OH-Chol-liposomes, but could not monitor the hydration in PEGylated OH-Chol-liposomes because PEG layers may cover and extend the fluorescence of laurdan in the headgroups of cationic lipids. On the other hand, the measurement of dielectric relaxation time detected the hydration of both surfactant-modified OH-Chol-liposomes and PEGylated OH-Chol-liposomes because the dielectric relaxation time of water revealed total hydration including hydration of the PEG layer and the headgroups of cationic lipids. This is the first report that dielectric relaxation time is a useful parameter for analysis of the hydration of liposomes and lipoplexes. These findings will help to select and provide optimal lipid formulations and surface modifications of liposomes, as well as optimal charge ratios of cationic liposomes and pDNA with fewer in vitro experiments.

Acknowledgements

This project was supported in part by the Open Research Center Project and by a grant for Research on Regulatory Science of Pharmaceuticals and Medical Devices from the Ministry of Health, Labor and Welfare.

References

Allen, T.M., Hansen, C.B., Lopes de Menezes, D.E., 1995. Pharmacokinetics of long circulating liposomes. Adv. Drug Deliv. Rev. 16, 267–284.

Blume, G., Cevc, G., 1990. One of the first publications demonstrating the prolonged circulation time of PEG-modified liposomes. Biochim. Biophys. Acta 1029, 91–97.

Ding, W., Hattori, Y., Qi, X., Kitamoto, D., Maitani, Y., 2009a. Surface properties of lipoplexes modified with mannosylerythritol lipid-A and Tween 80 and their cellular association. Chem. Pharm. Bull. 57, 138–143.

Ding, W., Izumisawa, T., Hattori, Y., Qi, X., Kitamoto, D., Maitani, Y., 2009b. Non-ionic surfactant modified cationic liposomes mediated gene transfection in vitro and in the mouse lung. Biol. Pharm. Bull. 32, 311–315.

Garbuzenko, O., Barenholz, Y., Priev, A., 2005. Effect of grafted PEG on liposome size and on compressibility and packing of lipid bilayer. Chem. Phys. Lipids 135, 117–129.

Gjetting, T., Arildsen, N.S., Christensen, C.L., Poulsen, T.T., Roth, J.A., Handlos, V.N., Poulsen, H.S., 2010. *In vitro* and *in vivo* effects of polyethylene glycol(PEG)-modified lipid in DOTAP/cholesterol-mediated gene transfection. Int. J. Nanomed. 5, 371–383.

Hattori, Y., Kubo, H., Higashiyama, K., Maitani, Y., 2005. Folate-linked nanoparticles formed with DNA complexes in sodium chloride solution enhance transfection efficiency. J. Biomed. Nanotechnol. 1, 176–184.

Igarashi, S., Hattori, Y., Maitani, Y., 2006. Biosurfactant MEL-A enhances cellular association and gene transfection by cationic liposome. J. Controlled Release 112, 362–368.

Inoh, Y., Kitamoto, D., Hirashima, N., Nakanishi, M., 2001. Biosurfactants of MEL-A increase gene transfection mediated by cationic liposomes. Biochem. Biophys. Res. Commun. 289, 57–61.

Kitamoto, D., Yanagisawa, H., Haraya, K., Kitamoto, H.K., 1998. Contribution of a chain-shortening pathway to the biosynthesis of the fatty acids of mannosylerythritol lipid (biosurfactant) in the yeast *Candida antarctica*: effect of β-oxidation inhibitors on biosurfactant synthesis. Biotechnol. Lett. 20, 813–818.

Klibanov, A.L., Maruyama, K., Torchilin, V.P., Huang, L., 1990. Amphipathic polyethyleneglycols effectively prolong the circulation time of liposomes. FEBS Lett. 268, 235–237.

Luciani, P., Bombelli, C., Colone, M., Giansanti, L., Ryhänen, S.J., Säily, V.M., Mancini, G., Kinnunen, P.K., 2007. Influence of the spacer of cationic gemini amphiphiles on the hydration of lipoplexes. Biomacromolecules 8, 1999–2003.

Hirsch-Lerner, D., Barenholz, Y., 1999. Hydration of lipoplexes commonly used in gene delivery: follow-up by laurdan fluorescence changes and quantification by differential scanning calorimetry. Biochim. Biophys. Acta 1461, 47–57.

Meidan, V.M., Cohen, J.S., Amariglio, N., Hirsch-Lerner, D., Barenholz, Y., 2000. Interaction of oligonucleotides with cationic lipids: the relationship between electrostatics, hydration and state of aggregation. Biochim. Biophys. Acta 1464, 251–261.

Parasassi, T., De Stasio, G., Ravagnan, G., Rusch, R.M., Gratton, E., 1991. Quantitation of lipid phases in phospholipid vesicles by the generalized polarization of Laurdan fluorescence. Biophys. J. 60, 179–189.

Sato, T., Sakai, H., Sou, K., Buchner, R., Tsuchida, E., 2007. Poly(ethylene glycol)-conjugated phospholipids in aqueous micellar solutions: hydration, static structure, and interparticle interactions. J. Phys. Chem. B 111, 1393–1401.

Stepniewski, M., Pasenkiewicz-Gierula, M., Róg, T., Danne, R., Orlowski, A., Karttunen, M., Urtti, A., Yliperttula, M., Vuorimaa, E., Bunker, A., 2011. Study of PEGylated lipid layers as a model for PEGylated liposome surfaces: molecular dynamics simulation and Langmuir monolayer studies. Langmuir 27, 7788–7798.

Takeuchi, K., Ishihara, M., Kawaura, C., Noji, M., Furuno, T., Nakanishi, M., 1996. Effect of zeta potential of cationic liposomes containing cationic cholesterol derivatives on gene transfection. FEBS Lett. 397, 207–209.

Woodle, M.C., Matthay, K.K., Newman, M.S., Hidayat, J.E., Collins, L.R., Redemann, C., Martin, F.J., Papahadjopoulos, D., 1992. Versatility in lipid compositions showing prolonged circulation with sterically stabilized liposomes. Biochim. Biophys. Acta 113, 193–200.

Yang, J.P., Huang, L., 1997. Overcoming the inhibitory effect of serum on lipofection by increasing the charge ratio of cationic liposome to DNA. Gene Ther. 4, 950–960.

Yoshioka, S., Aso, Y., Otsuka, T., Kojima, S., 1995. Water mobility in poly(ethylene glycol)-, poly(vinylpyrrolidone)-, and gelatine-water systems, as indicated by dielectric relaxation time, spin-lattice relaxation time, and water activity. J. Pharm. Sci. 84, 1072–1077.

Pharm Res (2011) 28:3237–3247
DOI 10.1007/s11095-011-0512-8

RESEARCH PAPER

Effect of Sugars on the Molecular Motion of Freeze-Dried Protein Formulations Reflected by NMR Relaxation Times

Sumie Yoshioka • Kelly M. Forney • Yukio Aso • Michael J. Pikal

Received: 23 November 2010 / Accepted: 10 June 2011 / Published online: 25 June 2011

ABSTRACT

Purpose To relate NMR relaxation times to instability-related molecular motions of freeze-dried protein formulations and to examine the effect of sugars on these motions.

Methods Rotating-frame spin-lattice relaxation time ($T_{1\rho}$) was determined for both protein and sugar carbons in freeze-dried lysozyme-sugar (trehalose, sucrose and isomaltose) formulations using solid-state ^{13}C NMR.

Results The temperature dependence of $T_{1\rho}$ for the lysozyme carbonyl carbons in lysozyme with and without sugars was describable with a model that includes two different types of molecular motion with different correlation times (τ_c) for the carbon with each τ_c showing Arrhenius temperature dependence. Both relaxation modes have much smaller relaxation time constant (τ_c) and temperature coefficient (Ea) than structural relaxation and may be classified as β-relaxation and γ-relaxation. The τ_c and Ea for γ-relaxation were not affected by sugars, but those for β-relaxation were increased by sucrose, changed little by trehalose, and decreased by isomaltose, suggesting that the β-mobility of the lysozyme carbonyl carbons is decreased by sucrose and increased by isomaltose.

Conclusion $T_{1\rho}$ determined for the lysozyme carbonyl carbons can reflect the effect of sugars on molecular mobility in lysozyme. However, interpretation of relaxation time data is complex and may demand data over an extended temperature range.

S. Yoshioka (✉) • K. M. Forney • M. J. Pikal
School of Pharmacy, University of Connecticut
Storrs, Connecticut 06269–3092, USA
e-mail: sumie.yoshioka@uconn.edu

Y. Aso
National Institute of Health Sciences
Setagaya, Tokyo 158–8501, Japan

KEY WORDS freeze-dried protein · molecular dynamics · NMR · relaxation time · sucrose

INTRODUCTION

Many researchers have recognized that the instability of pharmaceutical formulations in the amorphous state is correlated with the molecular dynamics (1–9). Correlations between instability and structural relaxation (10–18) or molecular motions with shorter timescales (β-relaxation or fast dynamics) (19–24) have been demonstrated for various amorphous formulations. For stability prediction and stabilization of freeze-dried protein (and labile small molecule) formulations, it is important to identify the motion most relevant to the instability, which largely depends on the degradation mechanisms and formulation components.

Various techniques have been used to determine molecular motions in amorphous formulations for proteins and small molecules. Structural relaxation has been characterized by dynamic mechanical measurements (25–27), isothermal microcalorimetry (28), differential scanning calorimetry (29), dielectric relaxation spectroscopy (30–32) and thermally stimulated depolarization current spectroscopy (33). Some of these techniques have also been used to characterize molecular dynamics on timescales shorter than structural relaxation. Fast dynamics of amorphous formulations on timescales much shorter than structural relaxation have been studied by neutron scattering and NMR relaxation measurements. Neutron scattering can probe atomic motions on the timescale of nanoseconds or shorter in freeze-dried formulations (22,23,34). NMR can detect atomic motions on the timescale of MHz and kHz, which are reflected by spin-lattice relaxation times in the

laboratory and rotating frames (T_1 and $T_{1\rho}$), respectively (35–37).

Although one might intuitively expect that instability of formulations would correlate best with structural relaxation because of the similar timescales of degradation and structural relaxation, correlations are often better with fast dynamics (20,22–24). For example, it has been demonstrated that NMR relaxation times T_1 and $T_{1\rho}$ are coupled with the instability of freeze-dried protein formulations. The $T_{1\rho}$ of the carbonyl carbons of freeze-dried insulin was increased by the addition of trehalose, which increased the storage stability of insulin (20). Sucrose, which increased the $T_{1\rho}$ of the protein carbonyl carbons more intensely than trehalose and stachyose, stabilized freeze-dried β-galactosidase more effectively than the others (24). These findings qualitatively suggest couplings between NMR fast dynamics and instability of freeze-dried protein formulations, but the mechanism of coupling is still unclear.

The purpose of this study is to quantify the timescales of molecular motions that are potentially coupled with instability and to elucidate the effect of sugars on these molecular motions. Here, $T_{1\rho}$ was determined for both protein and sugar carbons in freeze-dried protein formulations as a function of temperature using solid-state ^{13}C NMR. $T_{1\rho}$ is a NMR relaxation time, which does not directly indicate molecular mobility. Thus, the correlation time (τ_c) of the carbon, which indicates the time required for the carbon to rotate one radian, was determined from the temperature dependence of the observed $T_{1\rho}$. Trehalose, sucrose and isomaltose were used as excipients, and the well-studied protein lysozyme was used. Trehalose and sucrose are known to stabilize many freeze-dried proteins (20,24). Isomaltose is also a dissacharide with a similar molecular structure to trehalose and sucrose and has a T_g value between those of trehalose and sucrose. The effect of sugars on the τ_c of the carbon is discussed in relation to the stabilizing effects of these sugars. Furthermore, the temperature coefficient (apparent activation energy, Ea) of molecular motions is determined from the temperature dependence of τ_c and compared with the values reported for Ea as determined by other relaxation techniques, such as dynamic mechanical measurements, isothermal microcalorimetry and dielectric relaxation spectroscopy.

MATERIALS AND METHODS

Preparation of Freeze-Dried Formulations

Sucrose (S-9378, Sigma Chemical Co., St. Louis, MO, USA), trehalose (Pfanstiehl, Waukegan, IL, USA), isomaltose (400480–2 Seikagaku baio bijinesu Co., Tokyo, Japan) and ^{13}C-methyl isomaltose were freeze-dried with or without lysozyme (Sigma Chemical Co., St. Louis, MO, USA). ^{13}C-methyl isomaltose was prepared by methylating isomaltose with ^{13}C-methyl iodide (99% ^{13}C, Cambridge Isotope Laboratories, Inc., Andover, MA) using dimsyl sodium as a proton removal reagent (38).

Protein solutions (50 mg/mL) were prepared after dialysis against water. Protein : sugar solutions were prepared in a one-to-one ratio by diluting the protein solution to 25 mg/mL. Samples were prepared in 5 ml tubing glass vials (1 mL fill volume) and freeze-dried in a FTS Durastop freeze-drier (FTS Kinetics, Stoneridge, NY). The shelf temperature during primary drying was set at −25°C and increased at 0.1°C/min to 40°C for secondary drying and held for 6 h. Chamber pressure throughout drying was set at 80mTorr, and in all cases product temperature was maintained below collapse temperature. Vials were sealed in the chamber under vacuum using Daikyo Florotec stoppers and stored at −20°C until use. The water content determined by the Karl Fisher method was less than 0.2%. The glass transition temperature (T_g) measured by differential scanning calorimetry (TA Instruments) was 73°C for sucrose, 114°C for trehalose, 101°C for isomaltose, 88°C for lysozyme-sucrose, 131°C for lysozyme-trehalose and 109°C for lysozyme-isomaltose.

Determination of $T_{1\rho}$ of Lysozyme Carbonyl and Sugar Carbons by ^{13}C Solid-State NMR

The freeze-dried sample was added to a 4 mm Zirconia MAS rotor with a Macor cap (Wilmad LabGlass, Vineland, NJ), firmly, with the packing tool in a glove bag purged with dry nitrogen (relative humidity < 2%).

The $T_{1\rho}$ of each lysozyme carbonyl carbon and sugar carbon was determined at nominal (set) temperatures ranging from −70°C to 150°C (actual sample temperature: −57.3°C to 130.7°C) using a ^{13}C CP/MAS NMR operating at a proton resonance frequency of 300 MHz (Bruker DMX 300). The software used was Xwinnmr 2.6. Spin-locking field was equivalent to 62.5 kHz (^1H 90° pulse length was 4.0 μs). The spinning speed was 10 kHz. The contact time was 1.0 ms, and the recycling delay was 5 s. The maximum length of the spin locking pulse was varied with the $T_{1\rho}$ value from 4 ms to 30 ms. Signals were obtained at five spin locking pulse lengths. Signal acquisition was performed for 4–5 h at each data point except for the measurements to examine changes in $T_{1\rho}$ during heating below the T_g. Temperature was calibrated using ^{207}Pb MAS spectra of solid lead nitrate, as previously reported (39).

The NMR spectrum obtained for freeze-dried lysozyme is shown in Fig. 1, and those for trehalose, sucrose,

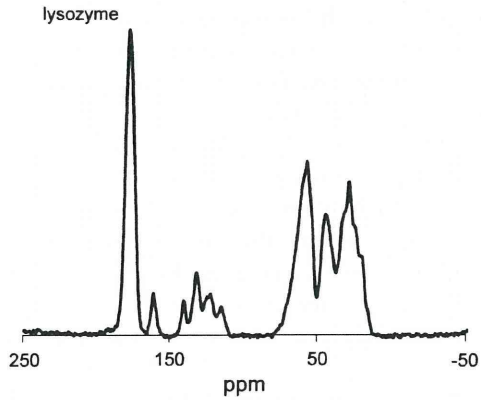

Fig. 1 NMR spectrum of freeze-dried lysozyme.

isomaltose, lysozyme-trehalose, lysozyme-sucrose and lysozyme-isomaltose are shown in Fig. 2. For the measurement of $T_{1\rho}$ for the lysozyme carbonyl carbons, the peak at approximately 175 ppm was used (observed $T_{1\rho}$ represents the average of that for all carbonyl carbons in all molecules of lysozyme). For the $T_{1\rho}$ measurement of trehalose carbon, the peak at 92 ppm belonging to the methine carbons (C-1 and C-1′) was used. The peak at 104 ppm belonging to the carbon (C-1) was used for the $T_{1\rho}$ measurement of sucrose carbon (40). For the $T_{1\rho}$ of isomaltose comprised of two anomers, the peak at 97 ppm, which mainly belongs to the methine carbon (C-1), was used. $T_{1\rho}$ was calculated by fitting the signal decay to a mono-exponential equation. τ_c was calculated from the $T_{1\rho}$ using the parameters estimated by fitting the $T_{1\rho}$ data to an equation describing the relationship between $T_{1\rho}$ and τ_c (described in the Discussion section) with the Origin 8.1 software (OriginLab Co., Northampton, MA).

Sub-T_g Heating of Freeze-Dried Lysozyme-Trehalose and Lysozyme-Sucrose

The effect of sub-T_g heating (i.e., annealing) on the $T_{1\rho}$ of the lysozyme carbonyl carbons was examined using freeze-dried lysozyme-trehalose and lysozyme-sucrose. Freeze-dried samples packed in the rotor were heated at 62°C for 8 h in the NMR probe with spinning at 10 kHz. Then, signal acquisition was started after temperature was lowered or raised to the target temperature.

In addition, the time dependence of changes in $T_{1\rho}$ during sub-T_g heating was examined by acquiring signals at −40°C, and then at 62°C, as a function of time. The duration required for a temperature change from −40°C to 62°C was 0.5 h. Signal acquisition at 62°C was started immediately after the temperature became constant and at intervals thereafter. Signal acquisition was carried out for 3 h at each time point.

RESULTS

Temperature Dependence for $T_{1\rho}$ of Lysozyme Carbonyl Carbons

The temperature dependence of the relaxation time is critical for the evaluation of the fundamental time constant, the molecular correlation time (τ_c). The time course of $T_{1\rho}$ relaxation for the carbonyl carbons of lysozyme was describable with the mono-exponential equation for all samples, both in the absence and the presence of sugars. Figure 3 shows the temperature dependence of the $T_{1\rho}$ calculated from the mono-exponential time course. The $T_{1\rho}$ of the carbonyl carbons in the absence of sugars and in the presence of trehalose and isomaltose exhibited a complex temperature dependence that shows two minima in the temperature ranges above 50°C and below 10°C, as well as a maximum at a temperature between 10°C and 90°C. For lysozyme freeze-dried with sucrose, $T_{1\rho}$ was not determined at temperatures above 90°C because of the possible complicating effects of a glass transition.

For the $T_{1\rho}$ minimum in the lower temperature range, the addition of sugars did not change the temperature at which the $T_{1\rho}$ minimum occurred. In contrast, for the $T_{1\rho}$ minimum in the higher temperature range, the minimum was impacted by the sugars with the effect of sugars on the temperature of $T_{1\rho}$ minimum varying with the sugar. Isomaltose significantly shifted the temperature of the $T_{1\rho}$ minimum to a lower temperature, whereas the effect of trehalose was not significant. Although the $T_{1\rho}$ minimum in the higher temperature range could not be directly observed for sucrose, sucrose shifted the temperature of the $T_{1\rho}$ maximum (which occurs between the two minima) to a higher temperature, suggesting that the $T_{1\rho}$ minimum is sifted to a higher temperature. Note also that the temperature of the $T_{1\rho}$ maximum was shifted to a lower temperature by isomaltose, whereas the effect of trehalose was not significant.

The value of $T_{1\rho}$ at the $T_{1\rho}$ minimum was increased by trehalose and isomaltose for both $T_{1\rho}$ minima in the lower and higher temperature ranges. Sucrose also increased the value of $T_{1\rho}$ at the $T_{1\rho}$ minimum in the lower temperature range. Trehalose exhibited the greatest effect on the $T_{1\rho}$ value at the minimum.

Effect of Sub-T_g Heating on $T_{1\rho}$ of Lysozyme Carbonyl Carbons

Annealing of freeze-dried formulations at temperatures below and near the T_g is well known to increase the α-relaxation time of the formulation (41). Thus, the change in $T_{1\rho}$ with time upon heating at a temperature below T_g was determined for the lysozyme carbonyl carbons in freeze-

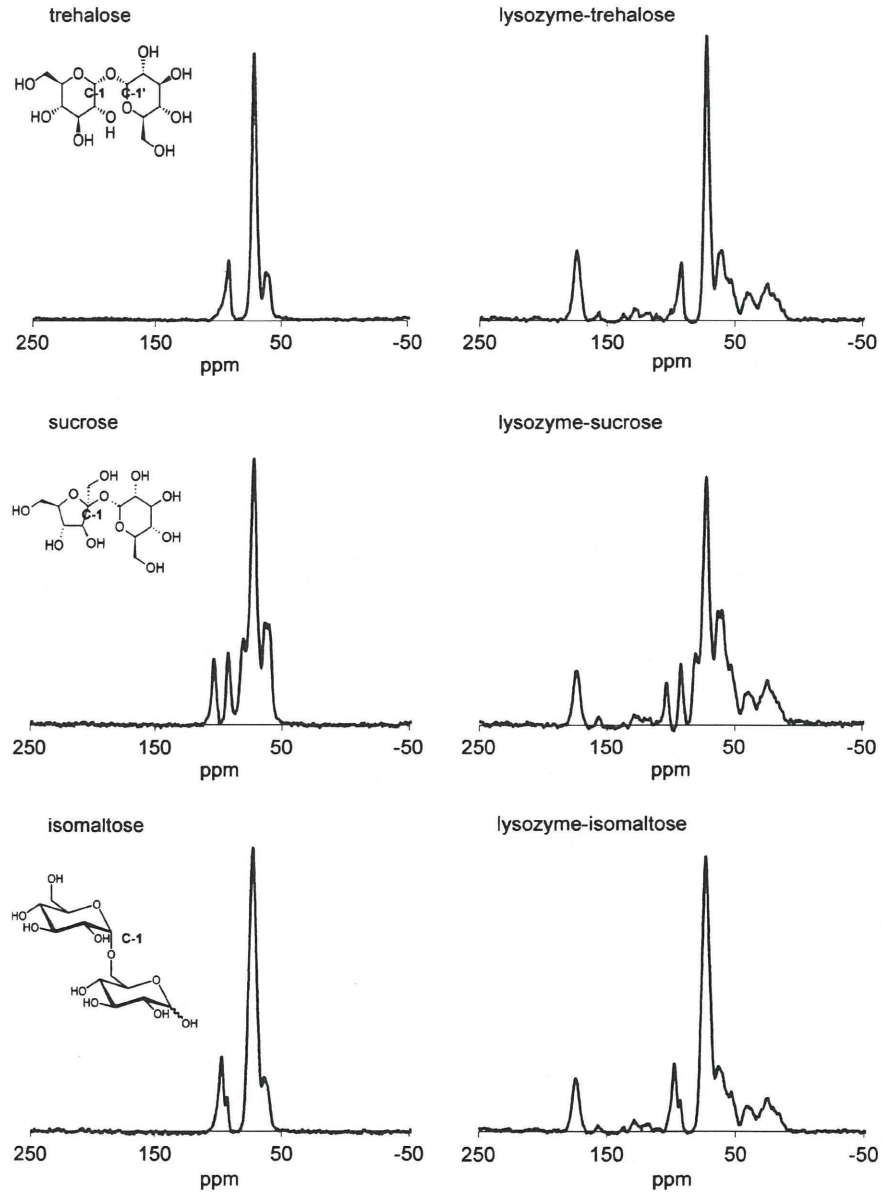

Fig. 2 NMR spectra of freeze-dried sugars and freeze-dried lysozyme with sugars.

dried lysozyme-trehalose and lysozyme-sucrose. Figure 4 shows the time dependence of changes in the $T_{1\rho}$ of the lysozyme carbonyl carbons associated with a temperature change from −40°C to 62°C. Similar changes were observed for both freeze-dried lysozyme-trehalose (Fig. 4a) and lysozyme-sucrose (Fig. 4b). Immediately after temperature was raised from −40°C to 62°C, $T_{1\rho}$ increased to a value similar to that determined at 62.3°C without the heating-cooling sequence, as shown in Fig. 3. Then, at a time shortly (≈ 3 hr) after the temperature rise, $T_{1\rho}$ sharply decreased. Thereafter, $T_{1\rho}$ gradually decreased further to an apparent equilibrium value.

Figure 5 compares the temperature dependence of $T_{1\rho}$ before and after heating at 62°C for 8 h. For both freeze-dried lysozyme-trehalose and lysozyme-sucrose, the values of $T_{1\rho}$ at temperatures above 0°C were greatly decreased by the heating treatment, whereas only small changes were observed at lower temperatures. The V-shaped temperature dependence of $T_{1\rho}$ observed for the sucrose system in the lower temperature range before heating was widened and the minimum moved toward higher temperature. For the trehalose system, the $T_{1\rho}$ minimum in the lower temperature range became obscure. We also found that the minimum in the high temperature range observed before heating was eliminated. These changes in $T_{1\rho}$ caused by sub-T_g heating indicate changes in the mobility of the carbon, the details of which will be described in the Discussion section.

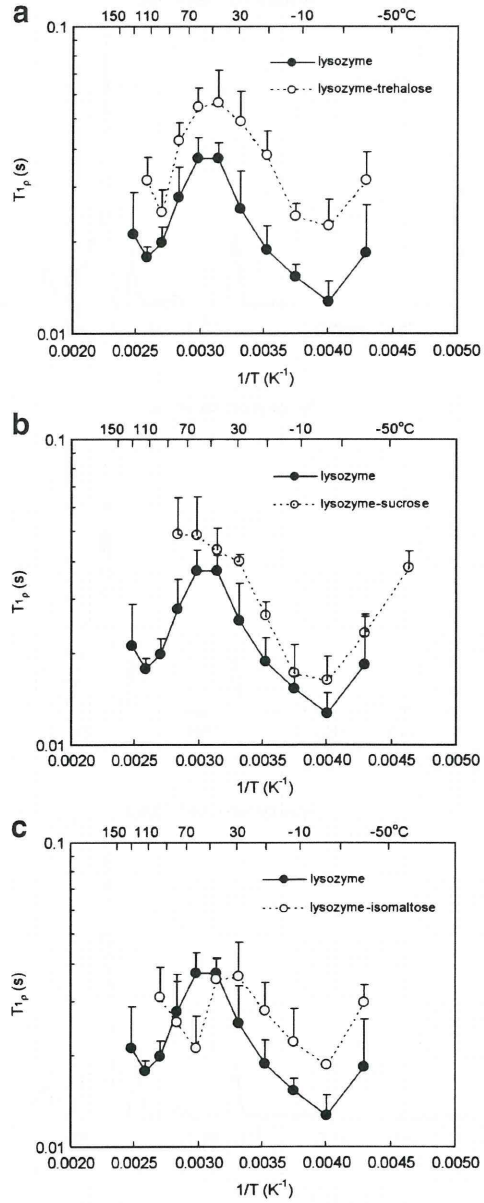

Fig. 3 Temperature dependence of $T_{1\rho}$ for lysozyme carbonyl carbons in freeze-dried lysozyme (**a**, **b**, **c**), lysozyme-trehalose (**a**), lysozyme-sucrose (**b**) and lysozyme-isomaltose (**c**) The error bars represent standard deviation ($n = 3$).

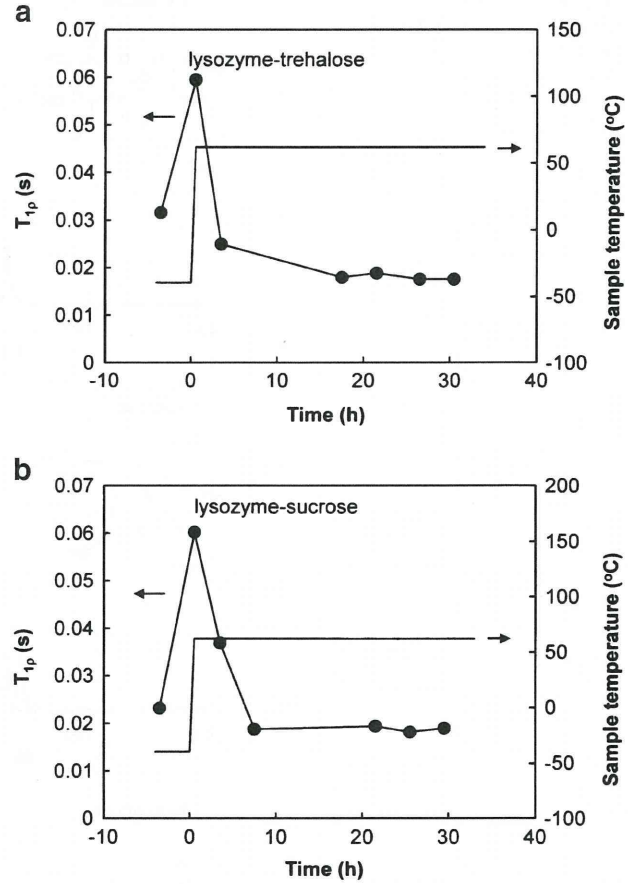

Fig. 4 Time dependence of changes in $T_{1\rho}$ of lysozyme carbonyl carbons in freeze-dried lysozyme-trehalose and lysozyme-sucrose. Temperature was increased from −40°C to 62°C at a time point of −0.5 h. The temperature reached 62°C at a time point of zero. Signal acquisition at 62°C was started at a time point of zero and at intervals thereafter. Signal acquisition was carried out for 3 h at each time point.

Temperature Dependence of $T_{1\rho}$ for Sugar carbon

The carbons of trehalose, sucrose and isomaltose (C-1 in Fig. 2) showed a peak separated from the peaks of the other methine carbons. Temperature dependence for the $T_{1\rho}$ of these carbons in the presence and absence of lysozyme is shown in Fig. 6 for the trehalose and sucrose carbons and in Fig. 7 for isomaltose. The addition of lysozyme did not bring about significant changes in the temperature dependence for the sugar carbons. The decrease in $T_{1\rho}$ observed in the high temperature range for the sucrose carbon was shifted to higher temperature by the addition of lysozyme most likely because of higher T_g of the lysozyme-sucrose system compared to the sucrose system.

Figure 7 also shows temperature dependence for the $T_{1\rho}$ of the methyl carbon introduced to the hydroxyl group of isomaltose. The methyl carbon exhibited a temperature dependence qualitatively similar to that of the methine carbon.

DISCUSSION

Mobility of Lysozyme Freeze-Dried with Sugars

The relationship between the correlation time τ_c and $T_{1\rho}$ of a given carbon can be described by Eq. 1, when